Establishment of a new nonalcoholic steatohepatitis model; Ovariectomy exacerbates nonalcoholic steatohepatitis -like pathology in diabetic rats

Yasuka Saigo[a,b], Tomohiko Sasase[a,b,*], Kinuko Uno[c], Yuichi Shinozaki[a,b], Tatsuya Maekawa[a], Ryuhei Sano[a,c], Yasufumi Toriniwa[a], Katsuhiro Miyajima[c], Takeshi Ohta[b]

a Biological/Pharmacological Research Laboratories, Takatsuki Research Center, Central Pharmaceutical Research Institute, Japan Tobacco Inc., 1-1 Murasaki-cho, Takatsuki, Osaka 569-1125, Japan

b Laboratory of Animal Physiology and Functional Anatomy, Graduate School of Agriculture, Kyoto University, Kitashirakawa Oiwake-cho, Sakyo-ku, Kyoto 606-8502, Japan

c Department of Nutritional Science and Food Safety, Faculty of Applied Biosciences, Tokyo University of Agriculture, 1-1-1 Sakuragaoka, Setagaya-ku, Tokyo 156-8502, Japan

Corresponding author*

Tomohiko Sasase, Ph.D.

Biological/Pharmacological Research Laboratories, Takatsuki Research Center, Central Pharmaceutical Research Institute, Japan Tobacco Inc., 1-1 Murasaki-cho, Takatsuki, Osaka 569-1125, Japan

E-mail address: tomohiko.sasase@jt.com (T. Sasase)

Abstract

An increasing number of patients worldwide are being diagnosed with nonalcoholic fatty liver disease and nonalcoholic steatohepatitis (NAFLD/NASH) because of the growing prevalence of obesity and metabolic disorders. The incidence of NAFLD is higher in postmenopausal women than in premenopausal women. The decline in the level of female hormones might have an effect on the deterioration of metabolism.

In the present study, we investigated the potential of Spontaneously Diabetic Torii (SDT) fatty rats as a new animal model for NAFLD. We created a menopausal model by ovariectomy (OVX) in female rats. Sprague-Dawley (SD) rats, SDT rats, and SDT-fatty rats were divided into sham and OVX groups and maintained until 40 weeks of age. The results showed that OVX-induced weight gain was observed in SD and SDT rats. In addition, OVX-induced hepatic triglyceride accumulation was increased in all strains, and there was a significant increase in hepatic triglyceride levels in OVX-SDT fatty rats compared to those in Sham-SD rats. Furthermore, liver fibrosis was worsened in the OVX-SDT fatty rats. In addition, OVX-induced increase in blood ALT level was observed in SDT-fatty rats. Gene expression analysis showed OVX-induced upregulation of *Srebp1* expression and

downregulation of *Pemt* and *Mttp* in OVX rats. These results indicate that OVX-SDT fatty rats exhibit NASH with more severe hepatic fibrosis than untreated animals, suggesting that OVX-induced estrogen reduction may have enhanced lipid synthesis in the liver. It is also possible, although hypothetical, that OVX may decrease VLDL secretion, which may more strongly induce NASH.

Keywords

NAFLD, NASH, SDT-fatty rats, ovariectomy (OVX)

Introduction

Nonalcoholic fatty liver disease (NAFLD) is a chronic liver disease, which has been diagnosed in an increasing number of patients worldwide. NAFLD is a continuum of non-alcoholic liver dysfunction ranging from simple steatosis to nonalcoholic steatohepatitis (NASH), and some of them progress to cirrhosis and liver cancer (Friedman et al., 2018). The majority of NAFLD patients have obesity, type 2 diabetes, and dyslipidemia; multiple factors (genetic, environmental, and epigenetic) are thought to influence disease development and progression, unlike in viral hepatitis and autoimmune liver diseases (Pais & Maurel, 2021). In recent years, in addition to these factors, age and sex differences have been considered factors responsible for the development of NAFLD. The prevalence and incidence of NAFLD tends to be higher in men than in premenopausal women (or those younger than 50–60 years), and higher in postmenopausal women (or those older than 50–60 years) (Lonardo et al., 2019). This difference in the incidence and prevalence of NAFLD based on sex and age might be because of the presence of male hormones or female hormonal changes due to menopause. In fact, in young women with NAFLD, higher testosterone levels are associated with a higher risk of NASH and NASH-induced liver fibrosis, as well as a high risk of abdominal fat (Sarkar et al., 2021). Furthermore, menopause is associated with changes in body composition, specifically with increased levels of intra-abdominal fat and increased waist circumference corrected for BMI, both of which are linked to an increased risk of metabolic diseases, including type 2 diabetes (DiStefano, 2020). *In vitro* studies using human hepatocytes have shown that 17-β-estradiol inhibits cell death, mitochondrial dysfunction, and triglyceride accumulation under NAFLD-like conditions, suggesting that it has hepatoprotective effects (Farruggio et al., 2020). In *in vivo*, non-obese male rats have decreased whole-body insulin sensitivity compared to female rats (Nadal-Casellas et al., 2012), and higher liver lipid accumulation when fed a high fat diet (HFD) (Stöppeler et al., 2013). There have been many reports on the influence of sex hormone differences on metabolic diseases, and as mentioned above, the same possibility has been suggested for NAFLD/NASH. There is evidence of protective effects of female hormones on hepatocytes and liver tissue at the *in vitro* and *in vivo* levels, which is consistent with the fact that the incidence of NASH in women increases after menopause.

The etiology and pathogenesis of NAFLD/NASH are complex, and not all of them are clear. Although

the gold standard for NASH animal models has not yet been established, a variety of models exist.

The SDT-fatty rat is a type 2 diabetes model in which a leptin receptor mutation is introduced into the genetic background of SDT rats. This mutation is an obesity gene in Zucker fatty rats. SDT-fatty rats show obesity, hyperglycemia, and hyperinsulinemia due to polyphagia at a young age (Masuyama et al., 2005), and female SDT-fatty rats show NASH-like symptoms at a high age without food loading (Ishii et al., 2015). Since many human patients with NAFLD are also obese and have type 2 diabetes mellitus (Tilg et al., 2017), we hypothesized that this model would be useful for studying the pathogenesis of NAFLD in humans. The ovariectomized (OVX) animal model is a postmenopausal female model that allows for NAFLD-like pathogenesis, such as steatosis and liver damage (Fukui et al., 2011; Kanaya et al., 2011). The main objective of this study was to investigate the possibility of using OVX-SDT fatty rats as a new NASH model by assessing the pathogenesis of NAFLD. For this purpose, we determined the pathological changes in the liver after OVX, measured the body weight, blood biochemical values, and lipid content of the liver, and evaluated the expression of lipid synthesis and fibrosis-related genes in the liver. OVX was also applied to SD rats as normal controls and SDT-fatty rats as genetic background controls, and various evaluations in the liver were performed.

Materials and Methods

Animals

Female SD rats, female SDT fatty rats, and female SDT rats were purchased from CLEA Japan Inc. (Tokyo, Japan). At 6 weeks of age, each rat lineage was divided into two groups ($n = 5$): a sham group and an ovariectomized (OVX) group. The animals were housed in a room climate-controlled for temperature (23 ± 3°C), humidity (55 ± 15%), and lighting (a 12 h dark-light cycle). All animals were fed a normal diet (CRF-1, Oriental Yeast Co., Ltd., Tokyo, Japan) and had free access to water. One animal in the SD rat sham group died during the experimental period, bringing the total number of animals in this group to $n = 4$. All remaining animals were necropsied at 40 weeks of age. All experimental protocols and animals were used according to strict compliance with our own laboratory guidelines for animal experimentation.

Tissue sampling and histopathological evaluation

Dissections were performed at 40 weeks of age. Animals were sacrificed by exsanguination under isoflurane anesthesia. The livers were sampled for determining the hepatic lipid content and analysis of mRNA expression and histopathology. The samples for liver lipid mass and mRNA analysis were frozen at -80°C until use. For pathological analysis, the livers were fixed in 10% neutral buffered formalin immediately after collection. The tissues were paraffin-embedded by standard techniques and

thin-sectioned (3 to 5 μm). For histopathological evaluation and liver fibrosis analysis, tissue sections were H&E stained and Sirius red stained, respectively. The Sirius red-positive area ratio was used as a liver fibrosis marker. Immunohistochemical examinations were conducted using antibodies against CD44 (Cell Signaling Technology, Inc., Danvers, MA, USA). Histofine Simple Stain Rat MAX-PO (MULTI) (Nichirei Bioscience Inc., Tokyo, Japan) was used as a secondary antibody, and the signals were visualized using 3,3′-diaminobenzidine (Wako Pure Chemical Industries, Ltd., Osaka, Japan).

Hepatic lipid contents

Approximately 100 mg of liver sections were taken in tubes, and zirconia beads and methanol (0.5 mL) were added. The samples were homogenized using a mixer mill (MM300 Retsch) (25 Hz, 10 min). To extract lipids from the homogenized solution, 1 mL of chloroform was added and mixed. All samples were then centrifuged (10,000 × *g*, 5 min, 4°C) and the supernatant (0.5 mL) was collected in other tubes and dried with nitrogen gas. The residue was dissolved in 0.5 mL 2-propanol. The TG, TC, and PL concentrations of the sample solutions were measured as fatty liver-related markers using a biochemistry automatic analyzer (Hitachi 7170S; Hitachi, Tokyo, Japan).

mRNA quantification

Total RNA was extracted from approximately 20 mg liver sections using the GenElute™ Mammalian Total RNA Miniprep Kit (MilliporeSigma, Burlington, Massachusetts, USA) according to the manufacturer's protocols. Reverse transcription was performed using the High-Capacity cDNA Reverse Transcription Kit with an RNase Inhibitor (Applied Biosystems, Foster City, California, USA) to synthesize complementary DNA (cDNA) from 1 μg of total RNA. For reverse transcription, the reaction mixture was incubated at 25°C for 10 min, 37°C for 120 min, and 85°C for 5 min. Gene expression was quantified using TaqMan Gene Expression Assays: Liver lipid-related genes: *Fasn* (Rn00569117_m1), *Scd1* (Rn06152614_s1), *Srebp1* (Rn01495769_m1), *Pemt* (Rn00564517_m1), *Mttp* (Rn01522963_m1); Fibrosis-related genes: *Col1a1* (Rn01463848_m1), *Acta2* (Rn01759928_g1), *Tgfb1* (Rn99999016_m1); Endogenous control gene: *Gapdh* (Rn99999916_s1). Real-time PCR was performed in a 10 μL reaction mixture contained 10 ng of cDNA with QuantStudio 7 Flex (Thermo Fisher Scientific, Waltham, Massachusetts, USA). The cycle parameters included 10 min at 95°C followed by 40 cycles of 15 sec at 95°C and 60 sec at 60°C.

Biological parameters

Body weight was measured at 6, 8, 16, 24, 32, and 40 weeks of age. Blood samples were collected from the rat tail vein at the beginning of the study and before autopsy to measure the following blood biochemical parameters: glucose (GLU), insulin (INS), triglycerides (TG), total cholesterol (TC), phospholipid (PL), alanine aminotransferase (ALT), and aspartate aminotransferase (AST). GLU, TG,

TC, PL, ALT, and AST levels were measured using respective product kits (Roche Diagnostics, Tokyo, Japan) and an automatic analyzer (Hitachi). INS levels were measured using enzyme-linked immunosorbent assay (ELISA) kits (Morinaga Institute of Biological Science, Yokohama, Japan).

Statistical analysis

All values are expressed as the mean ± standard deviation (SD). Statistical analyses between groups were performed as follows: Student's t-test or Aspin-Welch's t-test was used to compare the means of the two groups. In the comparison of multiple groups, Bartlett's test was first used to test for equal variability among the groups. As a result of the Bartlett test, Dunnett's test was used if data followed homoscedasticity, and Kruskal-Wallis test, followed by Dunn's multiple comparisons test, was used as a nonparametric test method if samples had no equal variances. The criterion for a significant difference was set at $P < 0.05$.

Results

OVX-induced obesity was observed in SD and SDT rats; SD rats showed significant weight gain compared to sham from 16 weeks of age (10 weeks after OVX), which continued until autopsy (Fig. 1A), and SDT rats showed significant weight gain from 2 to 10 weeks after OVX. The body weight of the OVX group remained higher than that of the sham group until autopsy (no significant difference) (Fig. 1C). In contrast, SDT-fatty rats were more obese than SD and SDT rats throughout the study period, but no OVX-induced weight gain was observed in the same strain (Fig. 1B). This suggests that OVX-induced weight gain may be difficult to detect in SDT-fatty rats because they are extremely obese under normal conditions.

The liver weight per body weight of SDT-fatty rats tended to be greater than that of SD and SDT rats in the same treatment. In contrast, no increase in liver weight was observed in either strain of OVX rats (Fig. 2A). To evaluate lipid accumulation in the liver, hepatic TG, TC, and PL contents were measured in the liver sections. The liver TG content was markedly increased, and PL content was considerably decreased in the OVX group of SDT-fatty rats compared to that in the Sham group of SD rats (Fig. 2B–D).

The blood GLU, INS, TG, TC, and PL levels of SDT-fatty rats were significantly higher than those of SD rats at the beginning of the study, suggesting that they developed diabetes and abnormal lipid metabolism. AST and ALT levels, indicative of liver damage, were also significantly higher. No abnormalities were observed in the blood biochemical parameters of SDT rats of the same age, suggesting that they did not develop diabetes at the beginning of the study (Fig. 3). Blood chemistry

values at necropsy showed significantly higher levels of TG, TC, and PL in both Sham and OVX rats compared to those of the Sham group of SD rats (Fig. 3B–D). There was also a significant increase in ALT levels in the SDT-fatty OVX group (Fig. 3E). A significant increase in blood insulin levels was observed only in the sham group of SDT rats compared to those in SD rats (Fig. 3G). As an effect of OVX in SDT-fatty rats, blood TG, TC, and PL tended to decrease (though not significantly different).

Microphotographs of liver tissue with H&E stain are shown in Figure 4A. Fatty liver and hypertrophy of hepatocyte in SDT-fatty rats tended to be exacerbated by OVX (Table 1). As inflammation marker of liver, CD44 immunostaining was performed; however, inflammation was largely unaffected by OVX (Fig. 4B and Table 1). Liver fibrosis is an important index for assessing the disease prognosis in patients with NASH. Liver fibrosis was assessed by liver sections stained with Sirius Red. There was a significant increase in the area of hepatic fibrosis in OVX SDT-fatty and SDT rats compared to that in Sham rats. However, this change was not observed in OVX SD rats (Fig. 4D). In histopathological imaging, OVX of SDT-fatty rats showed fibrous extension from the central venous region of the lobules to the surrounding tissues, and OVX of SDT rats showed Sirius Red-positive areas in the tissues, whereas in SD rats, these changes were hardly observed in OVX rats (Fig. 4C). OVX-induced liver fibrosis was found to be progressive in an animal model with a diabetic background.

The mRNA levels of lipid-related genes (*Fasn*, *Scd1*, *Srebp1*, *Pemt*, and *Mttp*) and fibrosis-related genes (*Col1a1*, *Acta2*, and *Tgfb1*) in the liver were measured using real-time PCR (Fig. 5). Compared with that in the Sham rats, *Srebp1*, a lipid synthesis gene, was upregulated approximately two-fold in OVX of SDT fatty rats (Fig. 5C), and the expression of *Pemt*, a major PL synthase in the liver, and *Mttp*, which is involved in the secretion of very low-density lipoprotein (VLDL), was significantly decreased (Fig. 5D–E). In contrast, there was no change in the expression of fibrosis-related genes (Fig. 5F–H). In OVX SDT rats, *Fasn* and *Srebp1* mRNA expression was significantly upregulated, and *Scd1* also showed an upregulation trend ($P = 0.0626$) (Fig. 5A–C), while *Pemt* and *Mttp* mRNA levels were unchanged (Fig. 5D–E). These results showed that there was a difference in the profile of OVX-induced hepatic gene expression between SDT-fatty rats and SDT rats.

Discussion

NAFLD/NASH is a liver disease that has attracted increasing attention because of the recent increase in the number of patients worldwide. It is a major cause of hepatocellular carcinoma, and many animal models for studying its pathogenesis have been reported. There are three main types of animal models for NASH: dietary burden models, genetically modified models, and drug-induced models. Typical models of each type include the choline-deficient L-amino-defined (CDAA) diet model, leptin receptor-deficient (*db/db*) mice, and carbon tetrachloride (CCl4) model, respectively. The CDAA

dietary model is a useful model for drug evaluation because it shows extreme fatty liver and inflammation, and rapid pathogenesis of liver fibrosis and hepatocarcinoma (Okishio et al., 2020). However, this model does not show weight gain or insulin resistance (Kamada et al., 2007; Matsumoto et al., 2013), and is considered to have a different metabolic profile from human NASH, making it an incomplete surrogate model for human disease. *db/db* mice are deficient in leptin signaling owing to mutations in the leptin receptor gene, and spontaneously develop typical NAFLD-like pathology, including overeating, obesity, insulin resistance, and fatty liver (Ibrahim et al., 2016). However, additional stimulation with a high-fat diet or a methionine-choline-deficient diet is required to show the features of NASH. The ability of this model to lead to advanced fibrosis and hepatocellular carcinoma has not been adequately investigated. Repeated administration of CCl4 has become one of the most common approaches to create models of drug-induced liver fibrosis, and long-term oral administration of CCl4 results in significant hepatotoxicity with liver fibrosis, cirrhosis, and hepatocellular carcinoma (Scholten et al., 2015). This feature of CCl4 is used for the evaluation of anti-fibrotic drugs, but its use is limited by the fact that it does not exhibit obesity and deviates from human NASH pathology, and deaths occur with long-term administration. As described above, each animal model of NASH has its own advantages and disadvantages, and there is currently no model that can completely mimic human NASH.

In a previous study, SDT-fatty rats developed metabolic abnormalities including hyperglycemia and hyperinsulinemia at a young age, and there was no difference in the pathogenesis between males and females (Ishii et al., 2010), but the pathophysiological features of NASH with fibrosis were only observed in female SDT-fatty rats (Ishii et al., 2015). In the present study, we showed that OVX-induced deterioration of lipid metabolism and the resulting worsening of NASH pathology were observed through the measurement of blood biochemical values and lipid content in the liver, gene expression analysis, and fibrosis analysis of liver tissue. OVX SDT-fatty rats showed elevated liver TG content, elevated ALT, a marker of liver injury, and increased liver fibrosis area, which were significantly different from those of SD Sham rats. We focused on the reduction of lipid secretion from the liver as a mechanism of OVX-induced TG accumulation in the liver.

OVX in SDT-fatty rats showed a tendency to decrease blood TG, TC, and PL, which are components of VLDL secreted by the liver, at autopsy compared to Sham rats (Blasiole et al., 2007). PEMT plays an important role in PL biosynthesis in the liver. An OVX-induced decrease in *Pemt* was observed in SDT-fatty rats, and a downward trend was also observed in other rat strains. In *in vitro*, mRNA expression and enzymatic activity of PEMT are upregulated by 17β-estradiol stimulation (Resseguie et al., 2007), and in vivo, NASH models lacking PEMT have been reported to have a worse condition compared to wild-type (Nakatsuka et al., 2016). In SDT-fatty rats, PL synthesis in the liver might be suppressed by the OVX-induced reduction of female hormone levels. In addition, *Mttp* mRNA levels were decreased in both Sham and OVX rats of SDT-fatty rats compared to those in Sham of SD rats.

MTP is involved in VLDL secretion from the liver and is downregulated by OVX in rats; additionally, it has been reported that estrogen supplementation restores *Mttp* mRNA expression in these animals (Barsalani et al., 2010). In other words, the synthesis of PL, the substance of VLDL, is suppressed in OVX of SDT-fatty rats, and lipid accumulation in the liver might be aggravated by the suppression of VLDL secretion due to the decrease in MTP.

An important feature of NASH pathology is inflammation of the liver as well as steatosis. In many studies of animal models of NASH, evaluation of liver pathology and elevated inflammatory cytokines have confirmed the establishment of NASH pathology. In this study, we evaluated liver inflammation and found no effect of OVX on mRNA expression of pro-inflammatory cytokines or inflammatory cell infiltration into the liver. Liver fibrosis is an important prognostic indicator in NASH, and in this study, we observed increased liver fibrosis area in OVX SDT-fatty rats, but no elevation of fibrosis-related genes. Previous studies have shown that these inflammation- and fibrosis- related genes are not altered in female SDT-fatty rats at 40 weeks of age and are upregulated at earlier time points (Ishii et al., 2015). It is probable that hepatic inflammation and fibrosis developed before 40 weeks of age in the present study, and the secretion of pro-inflammatory cytokines and activation of fibrosis-promoting reaction were reduced as the disease progressed. This study focused on capturing the pathological changes of liver fibrosis as the most important feature of NASH pathogenesis, and long-term rearing was conducted. On the other hand, earlier observation may be necessary to capture inflammatory pathology and the expression of NASH-related genes in the liver. The timing of observation is critical for the use of this model, and further research is needed to determine the time point at which all NASH characteristics can be captured simultaneously.

OVX-induced increase in liver fibrosis area was also observed in SDT rats, the genetic background of SDT-fatty rats. In a previous study, female SDT rats showed only fatty liver histopathology at 40 weeks of age (Hata et al., 2012) and no liver fibrosis. Therefore, it is possible that the worsening of metabolic abnormalities caused by OVX affected the development of hepatic fibrosis. However, unlike SDT-fatty rats, SDT rats did not show OVX-induced changes in parameters characteristic of NASH, such as increased lipids in the liver and elevated blood ALT and AST levels at 40 weeks of age.

In the blood biochemistry at the beginning of the study, SDT rats showed slightly higher ALT and AST levels than SD rats, but not as high as SDT-fatty rats. The blood GLU, TG, and insulin levels were similar to those of SD rats. Gene expression in the liver showed that *Fasn* and *Srebp1* were strongly expressed in SDT rats compared to those in SDT-fatty rats, and the mRNA expression of the inflammatory cytokines *Tnf* and *Ccl2* was upregulated (data not shown). These characteristics suggest that the process of OVX-induced disease progression in SDT rats may be considerably different from that in SDT-fatty rats. Further studies are needed to elucidate the mechanism of OVX-induced liver fibrosis in SDT rats.

In conclusion, female SDT and SDT-fatty rats showed liver fibrosis with fatty liver at 40 weeks of age after OVX. Female SDT-fatty rats show NASH pathophysiology without any special treatment, but OVX further develops this pathology, suggesting that it may be an important NASH model.

Table 1 Histopathological findings in liver

	SD Sham				SD OVX					SDT Sham					SDT OVX					SDT-fatty Sham					SDT-fatty OVX				
	1	2	3	4	1	2	3	4	5	1	2	3	4	5	1	2	3	4	5	1	2	3	4	5	1	2	3	4	5
Hepatosteatosis (Vacuolation/Fatty change)	–	–	–	–	–	±	±	–	–	±	±	–	±	±	±	±	+	±	–	±	±	–	±	+	++	+	+	–	+
Hypertrophy of hepatocyte	–	–	–	–	–	–	–	–	–	±	–	–	–	±	±	–	+	±	–	–	–	–	±	+	+	+	+	–	+
Infiltration, inflammatory cells	–	–	–	–	–	–	±	±	–	±	–	–	–	–	–	–	–	–	–	–	±	–	–	–	–	–	–	–	±
Fibrosis	–	–	–	–	–	–	–	–	–	±	–	–	–	–	+	±	±	–	–	±	±	±	±	±	+	+	+	–	±

–; Negative, ±; Very slight, +; Slight, ++; Moderate, +++; Severe

Summary of pathological evaluation by H&E staining (hepatosteatosis and hypertrophy of hepatocyte), CD44 immunostaining (infiltration of inflammatory cell), and Sirius Red staining (fibrosis) are represented (n = 4–5).

Figure Captions

Figure 1 Changes in body weight in SD, SDT, and SDT-fatty rats

A: SD rats, B: SDT rats, C: SDT-fatty rats

Data are shown as mean ± SD (n = 4–5). #P < 0.05, ##P < 0.01, comparison with sham of each strain.

SD: Sprague-Dawley

SDT: spontaneously diabetic Torii

SDT-fatty: spontaneously diabetic Torii fatty

OVX: ovariectomized

Figure 2 Liver weight and liver lipid contents at 40 weeks of age in SD, SDT, and SDT-fatty rats

A: Liver weight, B: Liver TG, C: Liver TC, D: Liver PL

Data are shown as mean ± SD (n = 4–5). *P < 0.05, comparison with sham of SD rats.

TG: Triglyceride

TC: Total cholesterol

PL: Phospholipids

Figure 3 Blood biochemical values at the beginning and the end of the study in SD, SDT, and SDT-fatty rats

A: Plasma GLU, B: Plasma TG, C: Plasma TC, D: Plasma PL, E: Plasma ALT, F: Plasma AST, G: Plasma INS

Left panel: pre (6 weeks of age), Right panel: post (40 weeks of age)

Data are shown as mean ± SD (n = 4-5). *P < 0.05, *P < 0.01 Dunnett's multiple comparison with sham of SD rats. $$P$ < 0.05, $$$P$ < 0.01 Dunn's multiple comparison with sham of SD rats.

GLU: Glucose, TG: Triglyceride, TC: Total cholesterol, PL: Phospholipids, ALT: Alanine transaminase, AST: Aspartate transaminase, INS: Insulin

Figure 4 Histopathological changes in SD, SDT, and SDT-fatty rats at 40 weeks of age

A: H-E staining of liver sections. Scale bars: 100 μm. B: CD44 immunostaining of liver sections. Scale bars: 100 μm. C: Sirius Red staining of liver sections. Scale bars:100 μm, D: Sirius Red-positive area (%). Data are shown as mean ± SD (n = 4–5). $$$P$ < 0.01, Dunn's multiple comparison with sham of SD rats.

Figure 5 Expression of hepatic genes related to lipid synthesis, lipid secretion and fibrosis at 40 weeks of age of SD, SDT, and SDT-fatty rats

A: *Fasn*, B: *Scd1*, C: *Srebp1*, D: *Pemt*, E: *Mttp*, F: *Col1a1*, G: *Acta2*, H: *Tgfb1*

Data are shown as mean ± SD (n = 4–5). *P < 0.05, **P < 0.01 Dunnett's multiple comparison with sham of SD rats.

Fasn: Fatty acid synthase, *Scd1*: Stearoyl-CoA desaturase 1, *Srebp1*: Sterol regulatory element-binding protein-1c, *Pemt*: Phosphatidylethanolamine N-Methyltransferase, *Mttp*: Microsomaltriglyceride transfer protein, *Col1a1*: Collagen type I alpha 1, *Acta2*: Actin alpha 2, *Tgfb1*: Transforming growth factor-β

References

Barsalani, R., Chapados, N. A., & Lavoie, J.-M. (2010). Hepatic VLDL-TG production and MTP gene expression are decreased in ovariectomized rats: Effects of exercise training. *Hormone and Metabolic Research = Hormon- Und Stoffwechselforschung = Hormones Et Metabolisme*, *42*(12), 860–867. https://doi.org/10.1055/s-0030-1267173

Blasiole, D. A., Davis, R. A., & Attie, A. D. (2007). The physiological and molecular regulation of lipoprotein assembly and secretion. *Molecular BioSystems*, *3*(9), 608–619. https://doi.org/10.1039/b700706j

DiStefano, J. K. (2020). NAFLD and NASH in Postmenopausal Women: Implications for Diagnosis and Treatment. *Endocrinology*, *161*(bqaa134). https://doi.org/10.1210/endocr/bqaa134

Farruggio, S., Cocomazzi, G., Marotta, P., Romito, R., Surico, D., Calamita, G., Bellan, M., Pirisi, M., & Grossini, E. (2020). Genistein and 17β-Estradiol Protect Hepatocytes from Fatty Degeneration by Mechanisms Involving Mitochondria, Inflammasome and Kinases Activation | Cell Physiol Biochem. *Cellular Physiology & Biochemistry*, *54*(3), 401–416.

Friedman, S. L., Neuschwander-Tetri, B. A., Rinella, M., & Sanyal, A. J. (2018). Mechanisms of NAFLD development and therapeutic strategies. *Nature Medicine*, *24*(7), 908–922. https://doi.org/10.1038/s41591-018-0104-9

Fukui, M., Senmaru, T., Hasegawa, G., Yamazaki, M., Asano, M., Kagami, Y., Ishigami, A., Maruyama, N., Iwasa, K., Kitawaki, J., Itoh, Y., Okanoue, T., Ohta, M., Obayashi, H., & Nakamura, N. (2011). 17β-Estradiol attenuates saturated fatty acid diet-induced liver injury in ovariectomized mice by up-regulating hepatic senescence marker protein-30. *Biochemical and Biophysical Research Communications*, *415*(2), 252–257. https://doi.org/10.1016/j.bbrc.2011.10.025

Hata, T., Ohta, T., Ishii, Y., Sasase, T., Yamaguchi, T., Mera, Y., Miyajima, K., Tanoue, G., Sato, E., & Matsushita, M. (2012). *Elevated glucagon-like peptide-1 on a high-fat diet feeding prevents the incidence of diabetes mellitus in Spontaneously Diabetic Torii* Lepr^{fa} *rats*. *2012*. https://doi.org/10.4236/jdm.2012.22027

Ibrahim, S. H., Hirsova, P., Malhi, H., & Gores, G. J. (2016). Animal Models of Nonalcoholic Steatohepatitis: Eat, Delete, and Inflame. *Digestive Diseases and Sciences*, *61*(5), 1325–1336. https://doi.org/10.1007/s10620-015-3977-1

Ishii, Y., Motohashi, Y., Muramatsu, M., Katsuda, Y., Miyajima, K., Sasase, T., Yamada, T., Matsui, T., Kume, S., & Ohta, T. (2015). Female spontaneously diabetic Torii fatty rats develop nonalcoholic steatohepatitis-like hepatic lesions. *World Journal of Gastroenterology*, *21*(30), 9067–9078. https://doi.org/10.3748/wjg.v21.i30.9067

Ishii, Y., Ohta, T., Sasase, T., Morinaga, H., Ueda, N., Hata, T., Kakutani, M., Miyajima, K., Katsuda,

Y., Masuyama, T., Shinohara, M., & Matsushita, M. (2010). Pathophysiological analysis of female Spontaneously Diabetic Torii fatty rats. *Experimental Animals*, *59*(1), 73–84. https://doi.org/10.1538/expanim.59.73

Kamada, Y., Matsumoto, H., Tamura, S., Fukushima, J., Kiso, S., Fukui, K., Igura, T., Maeda, N., Kihara, S., Funahashi, T., Matsuzawa, Y., Shimomura, I., & Hayashi, N. (2007). Hypoadiponectinemia accelerates hepatic tumor formation in a nonalcoholic steatohepatitis mouse model. *Journal of Hepatology*, *47*(4), 556–564. https://doi.org/10.1016/j.jhep.2007.03.020

Kanaya, N., Kubo, M., Liu, Z., Chu, P., Wang, C., & Yate-Ching Yuan, S. C. (2011). Protective Effects of White Button Mushroom (Agaricus bisporus) against Hepatic Steatosis in Ovariectomized Mice as a Model of Postmenopausal Women. *PLOS ONE*, *6*(10), e26654. https://doi.org/10.1371/journal.pone.0026654

Lonardo, A., Nascimbeni, F., Ballestri, S., Fairweather, D., Win, S., Than, T. A., Abdelmalek, M. F., & Suzuki, A. (2019). Sex Differences in Nonalcoholic Fatty Liver Disease: State of the Art and Identification of Research Gaps. *Hepatology*, *70*(4), 1457–1469. https://doi.org/10.1002/hep.30626

Masuyama, T., Katsuda, Y., & Shinohara, M. (2005). A Novel Model of Obesity-Related Diabetes: Introgression of the *Lepr*^{fa} Allele of the Zucker Fatty Rat into Nonobese Spontaneously Diabetic Torii (SDT) Rats. *Experimental Animals*, *54*(1), 13–20. https://doi.org/10.1538/expanim.54.13

Matsumoto, M., Hada, N., Sakamaki, Y., Uno, A., Shiga, T., Tanaka, C., Ito, T., Katsume, A., & Sudoh, M. (2013). An improved mouse model that rapidly develops fibrosis in non-alcoholic steatohepatitis. *International Journal of Experimental Pathology*, *94*(2), 93–103. https://doi.org/10.1111/iep.12008

Nadal-Casellas, A., Proenza, A. M., Lladó, I., & Gianotti, M. (2012). Sex-dependent differences in rat hepatic lipid accumulation and insulin sensitivity in response to diet-induced obesity. *Biochemistry and Cell Biology = Biochimie Et Biologie Cellulaire*, *90*(2), 164–172. https://doi.org/10.1139/o11-069

Nakatsuka, A., Matsuyama, M., Yamaguchi, S., Katayama, A., Eguchi, J., Murakami, K., Teshigawara, S., Ogawa, D., Wada, N., Yasunaka, T., Ikeda, F., Takaki, A., Watanabe, E., & Wada, J. (2016). Insufficiency of phosphatidylethanolamine N-methyltransferase is risk for lean non-alcoholic steatohepatitis. *Scientific Reports*, *6*, 21721. https://doi.org/10.1038/srep21721

Okishio, S., Yamaguchi, K., Ishiba, H., Tochiki, N., Yano, K., Takahashi, A., Kataoka, S., Okuda, K., Seko, Y., Liu, Y., Fujii, H., Takahashi, D., Ito, Y., Kamon, J., Umemura, A., Moriguchi, M., Yasui, K., Okanoue, T., & Itoh, Y. (2020). PPARα agonist and metformin co-treatment ameliorates NASH in mice induced by a choline-deficient, amino acid-defined diet with 45%

fat. *Scientific Reports*, *10*(1), 19578. https://doi.org/10.1038/s41598-020-75805-z

Pais, R., & Maurel, T. (2021). Natural History of NAFLD. *Journal of Clinical Medicine*, *10*(6). https://doi.org/10.3390/jcm10061161

Resseguie, M., Song, J., Niculescu, M. D., Costa, K.-A. da, Randall, T. A., & Zeisel, S. H. (2007). Phosphatidylethanolamine N-methyltransferase (PEMT) gene expression is induced by estrogen in human and mouse primary hepatocytes. *The FASEB Journal*, *21*(10), 2622–2632. https://doi.org/10.1096/fj.07-8227com

Sarkar, M. A., Suzuki, A., Abdelmalek, M. F., Yates, K. P., Wilson, L. A., Bass, N. M., Gill, R., Cedars, M., & Terrault, N. (2021). Testosterone is Associated With Nonalcoholic Steatohepatitis and Fibrosis in Premenopausal Women With NAFLD. *Clinical Gastroenterology and Hepatology*, *19*(6), 1267-1274.e1. https://doi.org/10.1016/j.cgh.2020.09.045

Scholten, D., Trebicka, J., Liedtke, C., & Weiskirchen, R. (2015). The carbon tetrachloride model in mice. *Laboratory Animals*, *49*(1 Suppl), 4–11. https://doi.org/10.1177/0023677215571192

Stöppeler, S., Palmes, D., Fehr, M., Hölzen, J. P., Zibert, A., Siaj, R., Schmidt, H. H.-J., Spiegel, H.-U., & Bahde, R. (2013). Gender and strain-specific differences in the development of steatosis in rats. *Laboratory Animals*, *47*(1), 43–52. https://doi.org/10.1177/0023677212473717

Tilg, H., Moschen, A. R., & Roden, M. (2017). NAFLD and diabetes mellitus. *Nature Reviews. Gastroenterology & Hepatology*, *14*(1), 32–42. https://doi.org/10.1038/nrgastro.2016.147

Figures

Figure 1

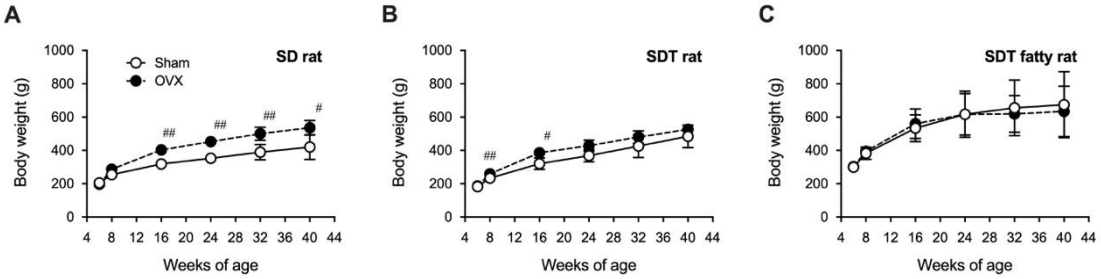

Figure 2

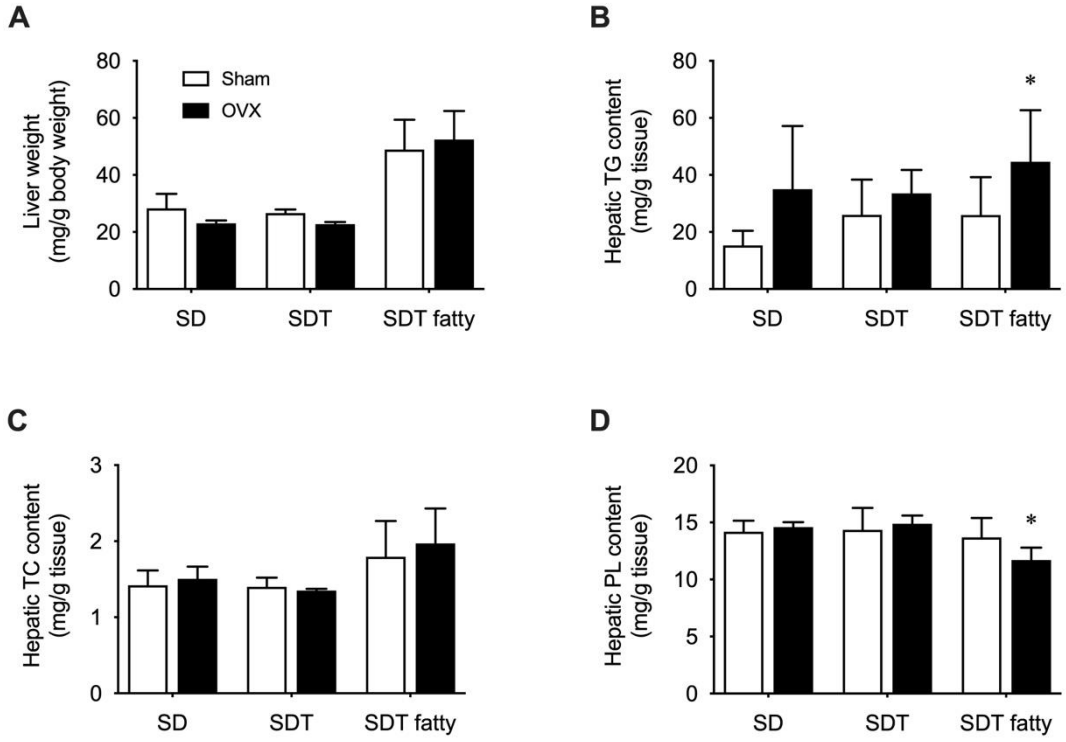
A
Liver weight (mg/g body weight)
Sham
OVX
80
60
40
20
0
SD
SDT
SDT fatty
B
Hepatic TG content (mg/g tissue)
*
C
Hepatic TC content (mg/g tissue)
3
2
1
D
Hepatic PL content (mg/g tissue)
20
15
10
5

Figure 3

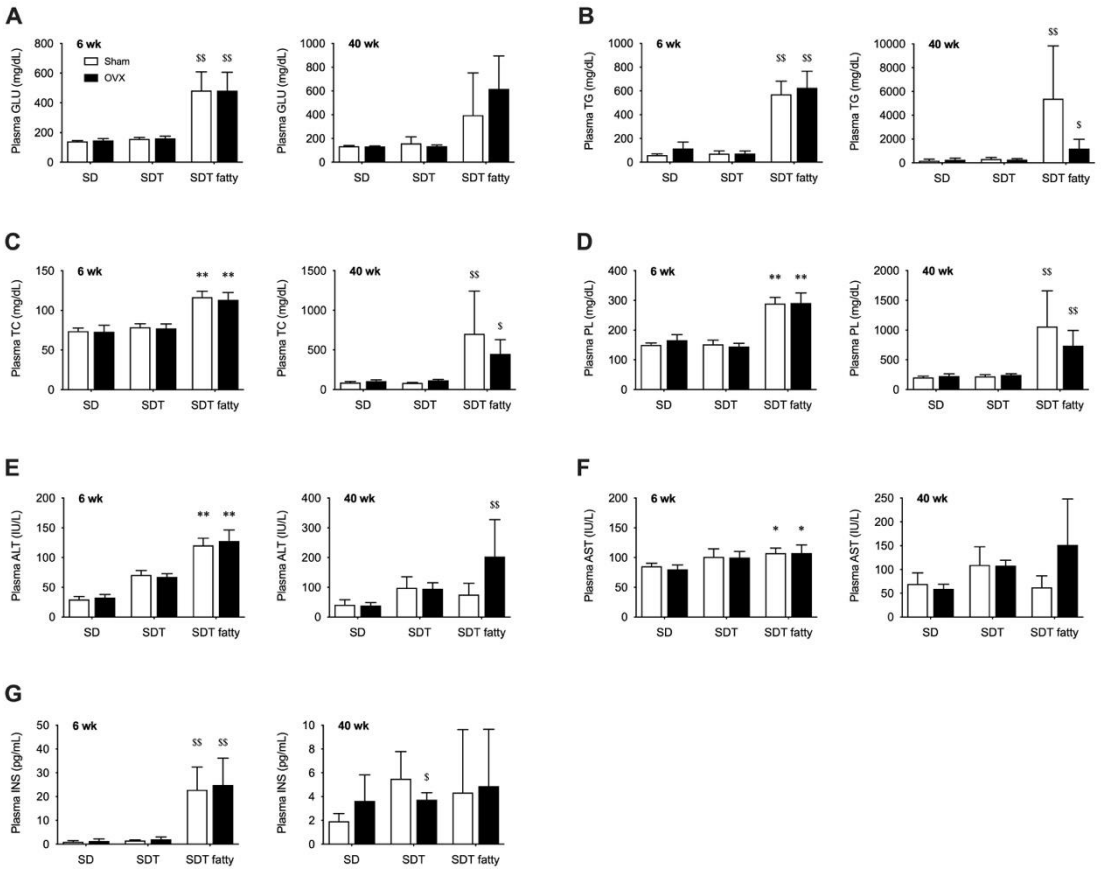
A
6 wk
Sham
OVX
Plasma GLU (mg/dL)
$$
$$
SD
SDT
SDT fatty
40 wk
B
Plasma TG (mg/dL)
C
Plasma TC (mg/dL)
**
$
D
Plasma PL (mg/dL)
E
Plasma ALT (IU/L)
F
Plasma AST (IU/L)
*
G
Plasma INS (pg/mL)

Figure 4

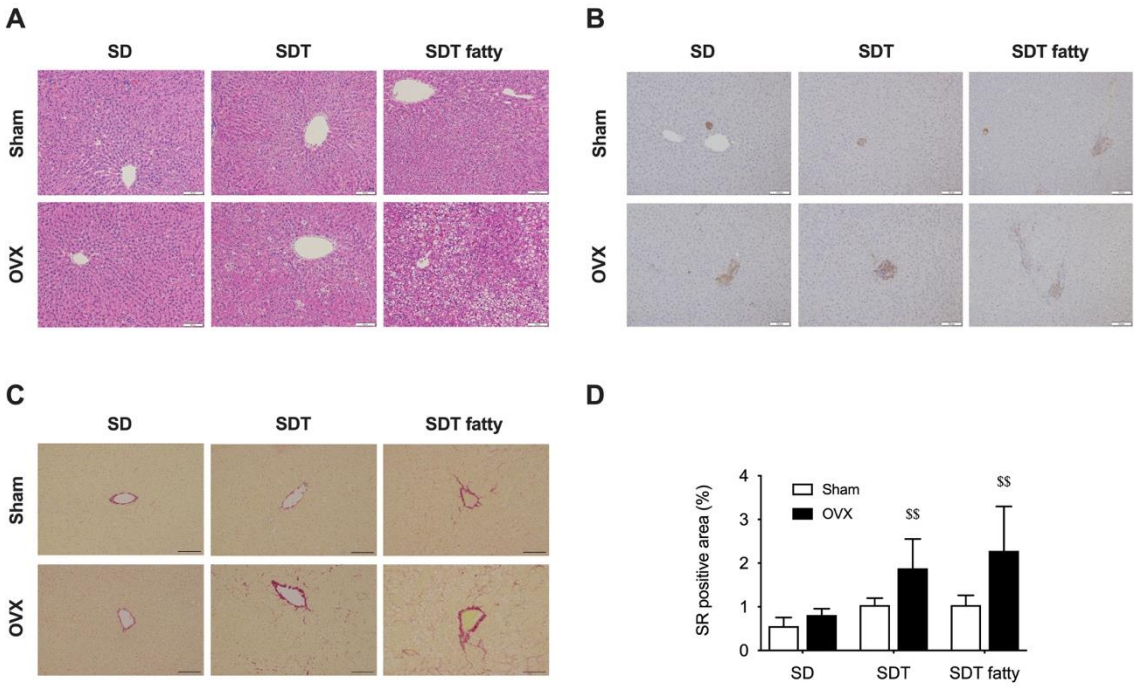
A
SD
SDT
SDT fatty
Sham
OVX
B
SD
SDT
SDT fatty
Sham
OVX
C
SD
SDT
SDT fatty
Sham
OVX
D
SR positive area (%)
Sham
OVX
$$
$$
0
1
2
3
4
SD
SDT
SDT fatty

Figure 5

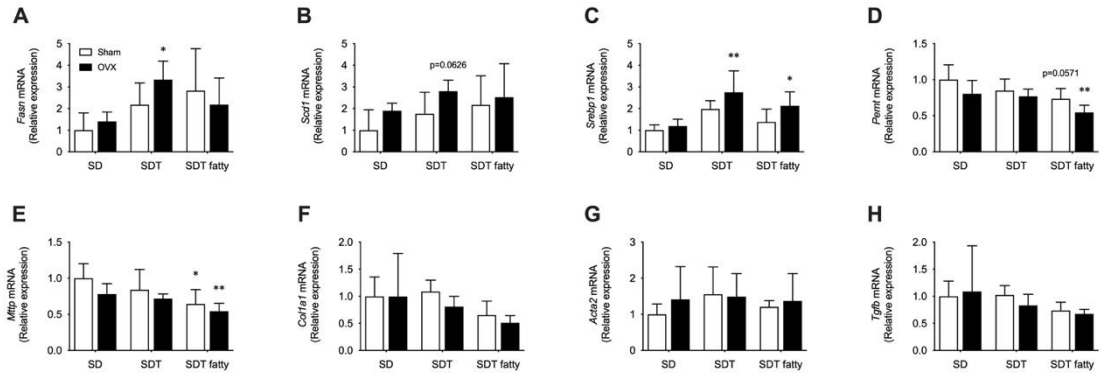
A
B
C
D
E
F
G
H
Sham
OVX
Fasn mRNA (Relative expression)
Scd1 mRNA (Relative expression)
Srebp1 mRNA (Relative expression)
Pemt mRNA (Relative expression)
Mttp mRNA (Relative expression)
Col1a1 mRNA (Relative expression)
Acta2 mRNA (Relative expression)
Tgfb mRNA (Relative expression)
p=0.0626
p=0.0571
SD
SDT
SDT fatty